

Hepatic Thermal Ablation: Effect of Device and Heating Parameters on Local Tissue Reactions and Distant Tumor Growth¹

Erik Velez, MD
S. Nahum Goldberg, MD
Gaurav Kumar, PhD
Yuanguo Wang, PhD
Svetlana Gourevitch, PhD
Jacob Sosna, MD
Tyler Moon, BS
Christopher L. Brace, PhD
Muneeb Ahmed, MD

Purpose:

To determine whether variable hepatic microwave ablation (MWA) can induce local inflammation and distant pro-oncogenic effects compared with hepatic radiofrequency ablation (RFA) in an animal model.

Materials and Methods:

In this institutional Animal Care and Use Committee–approved study, F344 rats (150 gm, $n = 96$) with subcutaneous R3230 breast adenocarcinoma tumors had normal non-tumor-bearing liver treated with RFA ($70^{\circ}\text{C} \times 5$ minutes), rapid higher-power MWA ($20\text{ W} \times 15$ seconds), slower lower-power MWA ($5\text{ W} \times 2$ minutes), or a sham procedure (needle placement without energy) and were sacrificed at 6 hours to 7 days (four time points; six animals per arm per time point). Ablation settings produced $11.4\text{ mm} \pm 0.8$ of coagulation for all groups. Distant tumor growth rates were determined to 7 days after treatment. Liver heat shock protein (HSP) 70 levels (at 72 hours) and macrophages (CD68 at 7 days), tumor proliferative indexes (Ki-67 and CD34 at 7 days), and serum and tissue levels of interleukin 6 (IL-6) at 6 hours, hepatocyte growth factor (HGF) at 72 hours, and vascular endothelial growth factor (VEGF) at 72 hours after ablation were assessed. All data were expressed as means \pm standard deviations and were compared by using two-tailed t tests and analysis of variance for selected group comparisons. Linear regression analysis of tumor growth curves was used to determine pre- and post-treatment growth curves on a per-tumor basis.

Results:

At 7 days, hepatic ablations with 5-W MWA and RFA increased distant tumor size compared with 20-W MWA and the sham procedure (5-W MWA: $16.3\text{ mm} \pm 1.1$ and RFA: $16.3\text{ mm} \pm 0.9$ vs sham: $13.6\text{ mm} \pm 1.3$, $P < .01$, and 20-W MWA: $14.6\text{ mm} \pm 0.9$, $P < .05$). RFA and 5-W MWA increased postablation tumor growth rates compared with the 20-W MWA and sham arms (preablation growth rates range for all arms: $0.60\text{--}0.64\text{ mm/d}$; postablation: RFA: $0.91\text{ mm/d} \pm 0.11$, 5-W MWA: $0.91\text{ mm/d} \pm 0.14$, $P < .01$ vs pretreatment; 20-W MWA: $0.69\text{ mm/d} \pm 0.07$, sham: $0.56\text{ mm/d} \pm 1.15$; $P = .48$ and $.65$, respectively). Tumor proliferation (Ki-67 percentage) was increased for 5-W MWA ($82\% \pm 5$) and RFA ($79\% \pm 5$), followed by 20-W MWA ($65\% \pm 2$), compared with sham ($49\% \pm 5$, $P < .01$). Likewise, distant tumor microvascular density was greater for 5-W MWA and RFA ($P < .01$ vs 20-W MWA and sham). Lower-energy MWA and RFA also resulted in increased HSP 70 expression and macrophages in the periablational rim ($P < .05$). Last, IL-6, HGF, and VEGF elevations were seen in 5-W MWA and RFA compared with 20-W MWA and sham ($P < .05$).

Conclusion:

Although hepatic MWA can incite periablational inflammation and increased distant tumor growth similar to RFA in an animal tumor model, higher-power, faster heating protocols may potentially mitigate such undesired effects.

¹From the Laboratory for Minimally Invasive Tumor Therapies, Department of Radiology, Beth Israel Deaconess Medical Center/Harvard Medical School, 1 Deaconess Rd, Boston, MA 02215 (E.V., S.N.G., G.K., Y.W., J.S., M.A.); Division of Image-guided Therapy and Interventional Oncology, Department of Radiology (S.N.G., J.S.), and Goldyne Savad Institute of Gene Therapy (S.G.), Hadassah Hebrew University Hospital, Jerusalem, Israel; and Departments of Radiology and Biomedical Engineering, University of Wisconsin–Madison, Madison, Wis (T.M., C.B.). Received October 11, 2015; revision requested December 17; revision received March 11, 2016; accepted April 11; final version accepted April 14. **Address correspondence to** M.A. (e-mail: mahmed@bidmc.harvard.edu).

Supported by a Radiological Society of North America Research Seed Grant (#1215), the Israel Research Foundation/Ministry of Health (no. 1277/15), and the National Cancer Institute (1U54CA151881-01). E.V. supported by Howard Hughes Medical Institute as a Howard Hughes Medical Institute–Society of Interventional Radiology Foundation Medical Research Fellow (no. 657892).

Thermal ablation with radiofrequency (RF) electrical current is used to treat a wide range of tumors in the liver, ranging from focal primary hepatocellular carcinoma (HCC) to metastatic colorectal and breast cancers (1–3). Advantages include lower associated morbidity and mortality compared with conventional surgery, use in patients who are not surgical candidates, and greater cost effectiveness (4,5). RF-based systems have been the standard thermal ablation modality for the treatment of focal tumors (5,6). However, to address challenges of achieving larger ablation zones and to overcome physiologic barriers, such as blood flow-induced heat sink effects, alternative thermal ablation platforms involving microwave (MW) energy have been actively developed and are gaining increased utility and clinical acceptance for tumor ablation (7,8). Potential advantages of MW ablation (MWA) that have led to its widespread use in clinical practice include the ability to generate higher tissue temperatures in shorter

durations that could potentially lead to larger coagulation zones (8).

Nonlethal hyperthermic injury that occurs as a byproduct of thermal ablation can incite a host of local tissue reactions within the periablational rim, including increased local heat shock protein (HSP) expression and downstream elevated levels of cytokines such as interleukin 6 (IL-6) within the serum (9,10). More recently, there is increasing clinical and experimental evidence that local periablational effects of RF ablation (RFA) contribute to systemic effects (“off-target” effects) that stimulate tumor development, growth, or more aggressive biology at separate sites within the same organ or in distant tumors (11–13). For example, Rozenblum et al (12,14) demonstrated that hepatic RFA can incite increased global liver regeneration and increased new tumor development in the *Mdr2* knockout model of chronic inflammatory cirrhosis and HCC tumorigenesis. Similarly, RFA of normal liver, which simulates the standard required clinical end point of achieving an ablative margin of 5–10 mm, can also stimulate distant subcutaneous breast tumors in a small-animal model (15).

Tissue responses within the periablational rim have been shown to vary according to ablative modality and thermal dose (16). Differences in various inflammatory markers, including interleukin-1 β , IL-6, and HSP 70, have been noted between RFA and MWA (9,10). Thus, it remains unclear to what

extent different thermal energy sources or the manner in which thermal energy is applied may contribute to (or, conversely, may be used to mitigate) the recently reported off-target tumorigenic effects of hepatic thermal ablation. Accordingly, the purpose of our study was to determine whether variable hepatic MWA can induce local inflammation and distant pro-oncogenic effects compared with hepatic RFA in an animal model.

Materials and Methods

Overview of Experimental Design

Approval of the institutional Animal Care and Use Committee was obtained for all studies. Our study was performed in three parts, for which a total of 96 Fischer 344 rats were used. Three different thermal ablation protocols were compared (lower-power, longer-duration MWA at 5 W for 120 seconds; higher-power, shorter-duration MWA at 20 W for 15 seconds; and RFA applied at 70°C for 5 minutes, each of which resulted in equivalently sized ablation



Advances in Knowledge

- Inflammation-mediated cytokine expressions after thermal ablation are in part based on the heating strategy selected rather than solely on the ablative energy source of microwave ablation (MWA) or radiofrequency ablation (RFA).
- Reduced local periablational inflammatory cellular infiltration and expression of interleukin 6 (IL-6), vascular endothelial growth factor (VEGF), and hepatocyte growth factor (HGF) were observed for higher-temperature, short-duration MWA compared with slower, lower-power MWA or RFA protocols ($P < .05$).
- Reduced distant tumor growth was also noted for higher-temperature, short-duration MWA compared with slower, lower-power MWA or RFA protocols ($P < .05$).

Implications for Patient Care

- For a given size ablation zone, thermal ablation algorithms can potentially be modified and tailored to modulate secondary periablational inflammation and distant tumorigenesis.
- Postablation hepatic inflammatory cell recruitment, hepatic and serum IL-6, HGF, and VEGF expression mirror increases in distant tumor growth and may be used as surrogate biomarkers to predict potential for distant tumor stimulation.

Published online before print

10.1148/radiol.2016152241 Content codes:  

Radiology 2016; 281:782–792

Abbreviations:

α -SMA = α -smooth muscle actin
 HCC = hepatocellular carcinoma
 HGF = hepatocyte growth factor
 HSP = heat shock protein
 IL-6 = interleukin 6
 MW = microwave
 MWA = MW ablation
 RF = radiofrequency
 RFA = RF ablation
 VEGF = vascular endothelial growth factor

Author contributions:

Guarantors of integrity of entire study, E.V., Y.W., M.A.; study concepts/study design or data acquisition or data analysis/interpretation, all authors; manuscript drafting or manuscript revision for important intellectual content, all authors; manuscript final version approval, all authors; agrees to ensure any questions related to the work are appropriately resolved, all authors; literature research, E.V., S.N.G., Y.W., J.S., M.A.; experimental studies, E.V., S.N.G., G.K., Y.W., S.G., T.M., C.B., M.A.; statistical analysis, E.V., S.N.G., Y.W., M.A.; and manuscript editing, E.V., S.N.G., Y.W., J.S., C.B., M.A.

Conflicts of interest are listed at the end of this article.

zones) in normal liver to simulate the standard clinical end point of ablating a margin of normal liver (12,17,18). A control arm of probe placement without applicator activation or ablation was also studied. First, the effects of the three hepatic ablation protocols on periablational inflammation and HSP 70 expression were compared at 24 hours after treatment (four arms with six animals each = 24 animals). Second, the effects of hepatic ablation protocol on cytokine (IL-6 at 6 hours) and growth factor (hepatocyte growth factor [HGF] and vascular endothelial growth factor [VEGF] at 72 hours) expression were compared (four arms with six animals each at two time points = 48 animals). IL-6 was measured 6 hours after ablation in periablational tissue and serum, while HGF and VEGF were measured 72 hours after ablation in periablational tissue, serum, and distant subcutaneous R3230 tumor (18,19). Additionally, α -smooth muscle actin (α -SMA)-positive hepatic stellate cell/activated myofibroblast presence in the periablational border zone was evaluated at 72 hours. Third, the effect of each hepatic ablation protocol on distant tumor growth was compared. R3230 breast adenocarcinoma tumors were implanted in situ in the mammary fat pads of Fischer 344 rats, and tumors were measured daily until they reached a mean diameter of 10–11 mm, at which point they were randomly assigned to one of four arms (four arms with six animals each = 24 animals). Tumor growth was measured daily for 7 days, followed by sacrifice and harvesting of the treated liver and distant tumor tissues. The primary outcome was the evaluation of tumor growth (tumor size and growth curve analysis comparisons), with secondary measurements of tumor proliferation (Ki-67), microvascular density (with CD34 staining), and macrophage accumulation (CD68 staining). Macrophage accumulation was also evaluated in nonablated liver and distant tumors.

Animal Models

For all experiments and procedures, anesthesia was induced with intraperitoneal injection of a mixture of

ketamine (50 mg per kilogram of body weight, Ketaject; Phoenix Pharmaceutical, St Joseph, Mo) and xylazine (5 mg/kg, Bayer, Shawnee Mission, Kan), and postprocedure analgesia was provided with standardized subcutaneous buprenorphine (0.3 mg/kg). Animals were sacrificed with an overdose of carbon dioxide (SMARTBOX CO2 Chamber System; EZ Systems, Palmer, Pa). In the first part of our study, Fischer 344 rats without tumors were used. In the second and third phases, experiments were performed in a well-characterized R3230 mammary adenocarcinoma model in which hepatic RFA leads to distant tumor growth (18,19). Cell lines were implanted subcutaneously in the mammary fat pads of female Fischer 344 rats (150 g \pm 20; 14–16 weeks old, Charles River, Wilmington, Mass). Tumor implantation, evaluation, and preparation techniques were performed as previously described (19). Briefly, one tumor was implanted into each animal by slowly injecting 0.3–0.4 mL of tumor suspension into the mammary fat pad of each animal with an 18-gauge needle. All animal studies were performed by several authors (E.V., G.K., Y.W., with 1–4 years of experience; supervised by M.A., with 16 years of experience).

Hepatic Thermal Ablation

Hepatic RFA was performed by using a conventional monopolar 500-kHz RFA generator (model 3E; Radionics, Burlington, Mass), as has been previously described (18,19). The liver was exposed by means of laparotomy using a subcostal incision in sterile conditions while the animal was anesthetized. The 1-cm tip of a 21-gauge electrically insulated electrode (SMK; Cosman Medical, Burlington, Mass) was placed in the liver. To complete the RF circuit, the animals were placed on a standardized metallic grounding pad (Radionics). RF energy was applied for 5 minutes with generator output titrated to maintain a designated tip temperature of 70°C \pm 2. Immediately after ablation, small quantities of saline were applied to wet the exposed tissue, preventing it from drying and adhering to the abdominal

wall after surgical closure. This standardized method of RF application has been previously demonstrated to provide reproducible coagulation volumes with the use of this conventional RFA system (18,19).

MWA procedures were performed in a similar fashion by using a single prototype dual-slot antenna (18 g) and a 8-GHz energy source (Emblation, Alloa, Scotland). The power and time combinations of 20 W for 15 seconds and 5 W for 120 seconds were optimized in preliminary studies to create reproducible coagulation volumes (11.4 mm \pm 0.4) that were similar in size and volume to those at RFAs (Fig 1). For sham treatments, the applicator was placed for 5 minutes, but no energy was administered, and the applicator was not connected to a generator. The MW applicator was used as the needle for sham studies. Results of prior studies have demonstrated that tumor growth rates were equivalent in control arms of laparotomy with needle placement alone or no surgery (19).

Tumor Growth Measurements

Tumors were measured in longitudinal and transverse diameters by using mechanical calipers, and an average diameter was calculated (E.V., G.K., Y.W.) (15). Measurements were taken every 1–2 days until the tumors reached 6–7 mm, at which point they were measured daily. Once tumors reached the target mean diameter of 10 mm, they were randomly allocated to treatment arms. After ablation or sham treatment, measurements were obtained daily for 7 days.

Quantification of IL-6, HGF, and VEGF

Serum and tissue samples (periablational and/or distant tumor, where specified) were harvested 6 hours after treatment for IL-6 and 72 hours after treatment for VEGF and HGF, as previous studies have demonstrated peak concentrations at these times (14,15,18). For liver samples, tissues were specifically harvested from the periablational rim. Samples were assayed for IL-6 (rat/R6000B Quantikine kit; R&D Systems, Minneapolis, Minn),

Figure 1

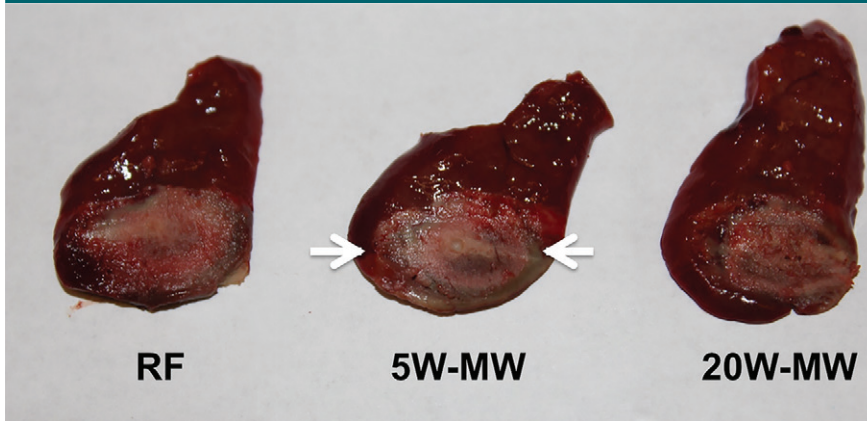


Figure 1: Optimization of low- and high-power MWA to create reproducible coagulation volumes similar to RFA. Animal livers were exposed by laparotomy using a subcostal incision. RF and MW probes were placed in the liver, and treatment was as follows: RFA (70°C × 5 minutes), longer-duration lower-power MWA (5 W × 2 minutes), or shorter-duration higher-power MWA (20 W × 15 seconds). Treatment areas (arrows) were reproducible and similar between all treatment groups.

HGF (rat/MHG00 Quantikine kit; R&D Systems), and VEGF (rat/RRV00 Quantikine kit; R&D Systems) by using an enzyme-linked immunosorbent assay, or ELISA, kit according to the manufacturer's instructions. Flash-frozen liver and tumor tissue was homogenized in a cold lysis buffer (Cell Signaling Technology, Beverly, Mass) consisting of 0.1% proteinase inhibitor (Sigma-Aldrich, St Louis, Mo). The homogenates were then centrifuged at 14000 rpm for 20 minutes at 4°C, and the total protein concentrations were determined by using a bicinchoninic acid method (Sigma-Aldrich). IL-6, VEGF, and HGF values were then normalized to protein concentration. Undiluted serum was used. All samples were measured in duplicate, and the average value was recorded (E.V., G.K., Y.W.) (19).

Immunohistochemistry

Histopathologic evaluation was performed on tissues from the primary site of liver ablation, from untreated liver tissue from the contralateral lobe where specified, and from distant subcutaneous tumors (E.V., G.K., Y.W., S.G., S.N.G., M.A.). All samples were fixed in 10% formalin for 48 hours at 4°C, embedded in paraffin blocks, and sliced at a thickness of 5 μm. Specimen

slides were imaged and analyzed by using a Micromaster I microscope (Fisher Scientific, Pittsburgh, Pa) and Micron Imaging Software (Westover Scientific, Mill Creek, Wash). Four random high-power fields were analyzed, for a minimum of three specimens per parameter. Immunohistochemical staining and quantification for macrophages (CD68, number of positive cells per high-power field) and HSP 70 (rim thickness) were performed to assess ablation-induced tissue responses, as has been described previously (12,18). On the basis of prior work demonstrating optimal detection with specific markers, immunohistochemical protocols were performed to assess proliferative indexes. CDC47 antibody was used to assess hepatocyte proliferation and liver regeneration (47DC141; Diagnostic BioSystems, Pleasanton, Calif), Ki-67 antibody was used to assess distant tumor cellular proliferation (Ab16667; Abcam, Cambridge, Mass), and CD34 was used to assess distant tumor microvascular density (AF4117, R&D Systems). For Ki-67 and CDC47, percentage cell positivity (ratio of positive cells to the sum of positive and negative cells) was calculated for each field and averaged for each sample. Quantification was performed for CD34

by counting the number of cells positive per high-power field.

Statistical Analysis

All data were expressed as means ± standard deviations. Selected mean tumor sizes (day 0 and at the time of sacrifice) and immunohistochemical quantifications were compared by using analysis of variance (ANOVA) with testing that included a posttreatment interaction term. Additional post-hoc analysis was performed with a two-sample, two-tailed Student *t* test if and only if the ANOVA achieved statistical significance. *P* < .05 was considered to indicate a significant difference. Tumor growth curves before and after treatment were analyzed by using linear regression analysis models to determine the slope of the pre- and posttreatment growth curves on a per-tumor basis. From these data, mean posttreatment growth curve slopes ± standard deviations were then calculated and compared by using ANOVA and paired two-tailed *t* tests.

Results

Comparison of Periablational Markers of Thermal Injury (ie, HSP 70) and Inflammatory Cell Recruitment

Cells staining positive for HSP 70 accumulated in the periablational zone in all three treatment arms. At 24 hours, the RFA and 5-W MWA treatment arms had increased expression of HSP 70 compared with the 20-W MWA treatment arm (Fig 2). The periablational rim thickness, as determined by HSP 70 expression, was similar between RFA (163.9 μm ± 8.6) and 5-W MWA (151.8 μm ± 13.7) but was significantly greater than that of 20-W MWA (87 μm ± 12.9, *P* < .01).

An increase in macrophages was seen in the periablational border zone for all ablation methods at 7 days (Fig 3). The number of macrophages was most elevated in the RFA arm, with significant differences seen between all treatment modalities and background normal liver from untreated sham-procedure animals (RFA: 40.4 ± 14.8; 5-W MWA: 29.5 ± 8.9; 20-W MWA: 16.3 ±

Figure 2

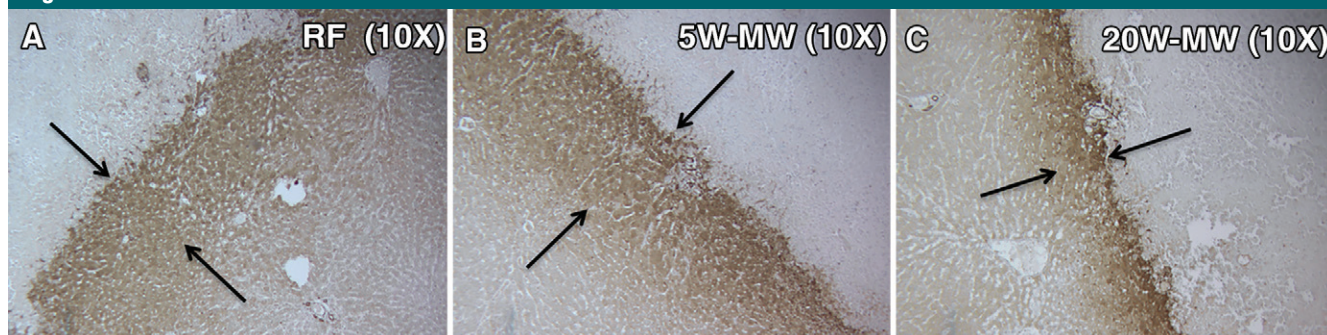


Figure 2: Effects of MWA and RFA on periablational rim thickness. Representative images of background liver stained for HSP 70. (Original magnification, $\times 10$.) Rats were treated with liver ablation with, *A*, RFA, *B*, lower-power, longer-duration 5-W MWA, and, *C*, higher-power, shorter-duration 20-W MWA. Rats were sacrificed, and tissues were stained 24 hours after treatment. Periablational rim thickness, as determined by HSP 70 expression, was seen in all treatment arms (arrows). As shown, rapid higher-power MWA produced a significantly smaller periablational zone than did RFA and lower-power MWA ($P < .01$).

5.2; sham: 4.9 ± 2.6 ; $P < .05$). Macrophages were also noted in the unablated liver lobe and in distant tumor. In the unablated liver lobe, there were fewer macrophages in the 20-W MWA treatment arm (2.5 ± 1.4) compared with the RFA (7.8 ± 1.8), 5-W MWA (5.8 ± 4.3), and sham-treatment (4.9 ± 2.6) arms ($P < .05$), with no other differences between arms noted. However, there was no significant difference in macrophages between treatment arms and the sham-treatment arm in the distant tumor (sham: 5.3 ± 2.4 ; RFA: 3.6 ± 1.8 ; 5-W MWA: 6.2 ± 2.3 ; 20-W MWA: 3.8 ± 3.1 ; $P > .05$).

In the liver, the number of cells entering mitosis (CDC-47, number of cells positive per high-power field) in the ablated lobe was highest for 5-W MWA (18.5 ± 13.9), followed by RFA (14.4 ± 7.0); both were significantly higher than that for 20-W MWA (1.6 ± 1.4 , $P < .01$). The number of CDC-47-positive hepatocytes in the unablated lobe was similarly elevated for RFA (17.9 ± 10.8); however, it was less prominent in 5-W MWA (3.1 ± 3.3), although it was significantly higher for both 5-W MWA and RFA than for 20-W MWA (0.7 ± 1.0 , $P < .05$). Additionally, the number of α -SMA-positive cells expressed in the periablational zone at 3 days was elevated in the 5-W MWA group (24.2 ± 10.3) compared with that in the 20-W MWA group (13.1 ± 5.0 , $P < .01$); however, no differences were seen between

Figure 3

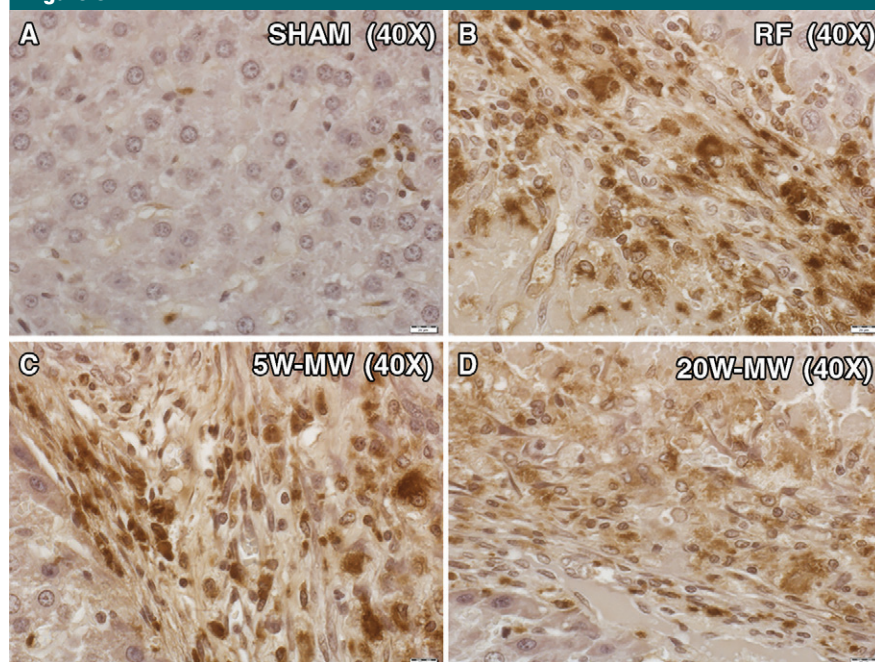


Figure 3: Macrophages in periablational zone after hepatic ablation. Representative images of background liver surrounding the ablation zone stained for macrophages (CD68). (Original magnification, $\times 40$.) Fisher rats were treated with liver ablation with RFA, lower-power MWA, or higher-power MWA. At day 7, the animals were sacrificed. Liver tissue was harvested in the periablational zone and was subsequently immunohistochemically stained for CD68 for assessment of macrophage infiltration. *B*, RFA and, *C*, lower-power MWA stimulated a higher number of macrophages to the periablational zone compared with, *A*, the sham procedure and, *D*, higher-power MWA ($P < .01$).

the 20-W MWA and RFA arms (RFA: 11.9 ± 6.8). There was no difference in α -SMA-positive cells in untreated liver between various treatment arms.

Growth Factor and Cytokine Elevation after Different Hepatic Ablations

Elevations of serum and periablational liver levels of IL-6 were seen in all

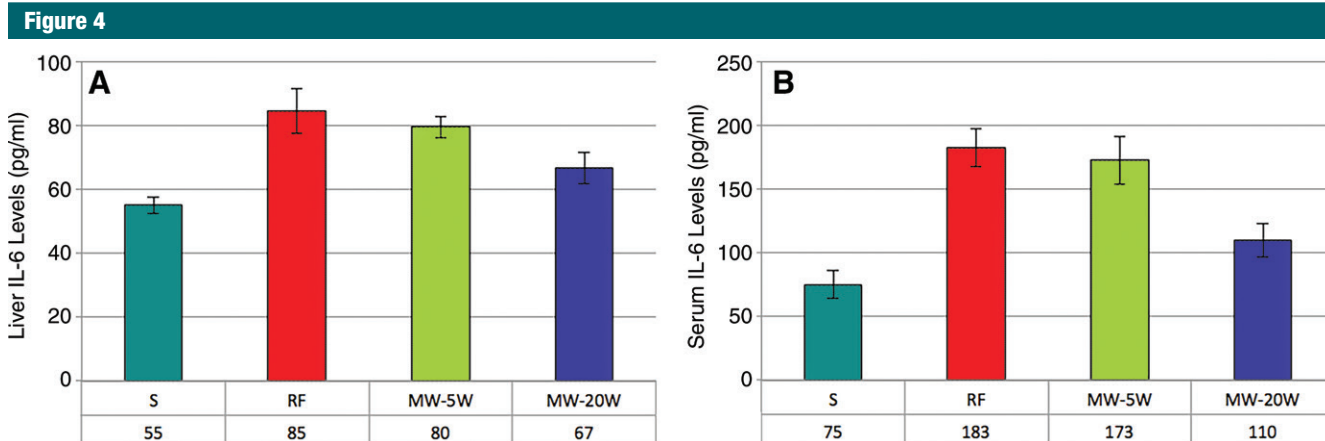


Figure 4: Bar graphs show, *A*, liver and, *B*, serum levels of IL-6 after ablation. Serum and liver IL-6 levels were determined by using an enzyme-linked immunosorbent assay, or ELISA, protocol in animals treated with RFA, lower-power MWA, or higher-power MWA liver ablation. Levels were tested 6 hours after ablation, and elevations in both liver and serum IL-6 were seen in all treatment arms 6 hours after ablation. Levels of IL-6 were significantly higher in the RFA and lower-power MWA groups than in the higher-power MWA group.

treated animals compared with sham-treated animals ($P < .05$) (Fig 4). The intrahepatic IL-6 levels in the vicinity of the border zone were significantly higher at 6 hours after treatment for RFA (80 pg/mL \pm 3) and 5-W MWA (80 pg/mL \pm 3) compared with both 20-W MWA (67 pg/mL \pm 5, $P < .05$) and untreated rats (55 pg/mL \pm 3, $P < .01$). Serum levels followed the same trend, with increased IL-6 concentrations in RFA and 5-W MWA compared with 20-W MWA and sham (RFA: 183 pg/mL \pm 15; 5-W MWA: 173 pg/mL \pm 19 vs 20-W MWA: 110 pg/mL \pm 13; and sham: 75 pg/mL \pm 11, $P < .01$), with a significant difference between the 20-W MWA and sham arms as well ($P = .03$). No differences in distant tumor IL-6 levels at 6 hours were seen between the treatment and sham arms.

Liver periablation zone levels of HGF were elevated in RFA (11224 pg/mL \pm 597) and 5-W MWA (12124 pg/mL \pm 1078) 72 hours after treatment compared with those in 20-W MWA (9445 pg/mL \pm 1850, $P < .01$) and sham (9156 pg/mL \pm 767, $P < .01$), with no significant difference between 20-W MWA and sham (Fig 5a). Tumor HGF levels were also increased for RFA and 5-W MWA compared with those for 20-W MWA and sham (RFA: 2897 pg/mL \pm 261; 5-W MW: 2813 pg/mL

\pm 219 vs 20-W MW: 1960 pg/mL \pm 208 and sham: 1924 pg/mL \pm 300, $P < .01$). However, no differences were seen in serum levels of HGF at 72 hours (Fig 5, *B*).

Tumor VEGF levels at 72 hours after treatment were elevated in all treatment arms compared with those in the sham-treatment arm ($P < .05$), with significantly lower levels of VEGF in 20-W MWA compared with RFA and 5-W MWA ($P < .05$) (RFA: 5170 pg/mL \pm 305, 5-W MWA: 5952 pg/mL \pm 1068, 20-W MWA: 3915 pg/mL \pm 881, sham: 2777 pg/mL \pm 119) (Fig 5, *D*). Very low levels of VEGF were seen in the livers of all groups (Fig 5, *C*), and serum levels of VEGF were undetectable.

Effect of Different Hepatic Ablation Protocols on Distant Tumor Growth

For the R3230 tumors, preoperative tumor sizes and growth rates were equivalent, at 9.8 mm/d \pm 0.8 and 0.61 mm/d \pm 0.07, respectively (Table). Hepatic ablation with RFA and low-power 5-W MWA increased the growth of the distant untreated subcutaneous tumor, resulting in significantly larger tumors at 7 days compared with sham (5-W MWA: 16.3 mm \pm 1.1; RFA: 16.3 mm \pm 0.9 vs sham: 13.6 mm \pm 1.3, $P < .01$). High-power 20-W MWA tumor growth (14.6 mm \pm 0.9) was significantly lower than both low-power

5-W MWA and RFA tumor growth ($P < .05$) and was not significantly different from that in sham-treated animals ($P = .15$) (Fig 6). Additionally, RFA and 5-W MWA increased tumor growth rates after treatment (preablation growth slopes: RFA: 0.60 mm/d \pm 0.07; 5-W MWA: 0.62 mm/d \pm 0.07; postablation slopes: RFA: 0.91 mm/d \pm 0.11; 5-W MWA: 0.91 mm/d \pm 0.14; $P < .01$), whereas no significant difference was seen in 20-W MWA or untreated liver (preablation growth slopes: sham: 0.60 mm/d \pm 0.11; 20-W MWA: 0.64 mm/d \pm 0.02; postablation slopes: sham: 0.56 mm/d \pm 1.15; 20-W MWA: 0.69 mm/d \pm 0.07; $P = .48$ and $P = .65$, respectively).

In the distant R3230 tumors, increased cellular proliferation (Ki-67, percentage cell positivity per high-power field) was observed in all treatment groups compared with the sham treatment group (49% \pm 5, $P < .01$) at 7 days after treatment (Fig 7). Additionally, a statistically significant increase in the amount of cells undergoing mitosis was seen in RFA (79% \pm 5) and 5-W MWA (82% \pm 5) compared with 20-W MWA (65% \pm 2, $P < .01$). Increases in distant tumor microvascular density (CD34 staining, number of vessels positive per high-power field) were also observed for RFA and 5-W MWA compared with 20-W MWA and

Figure 5

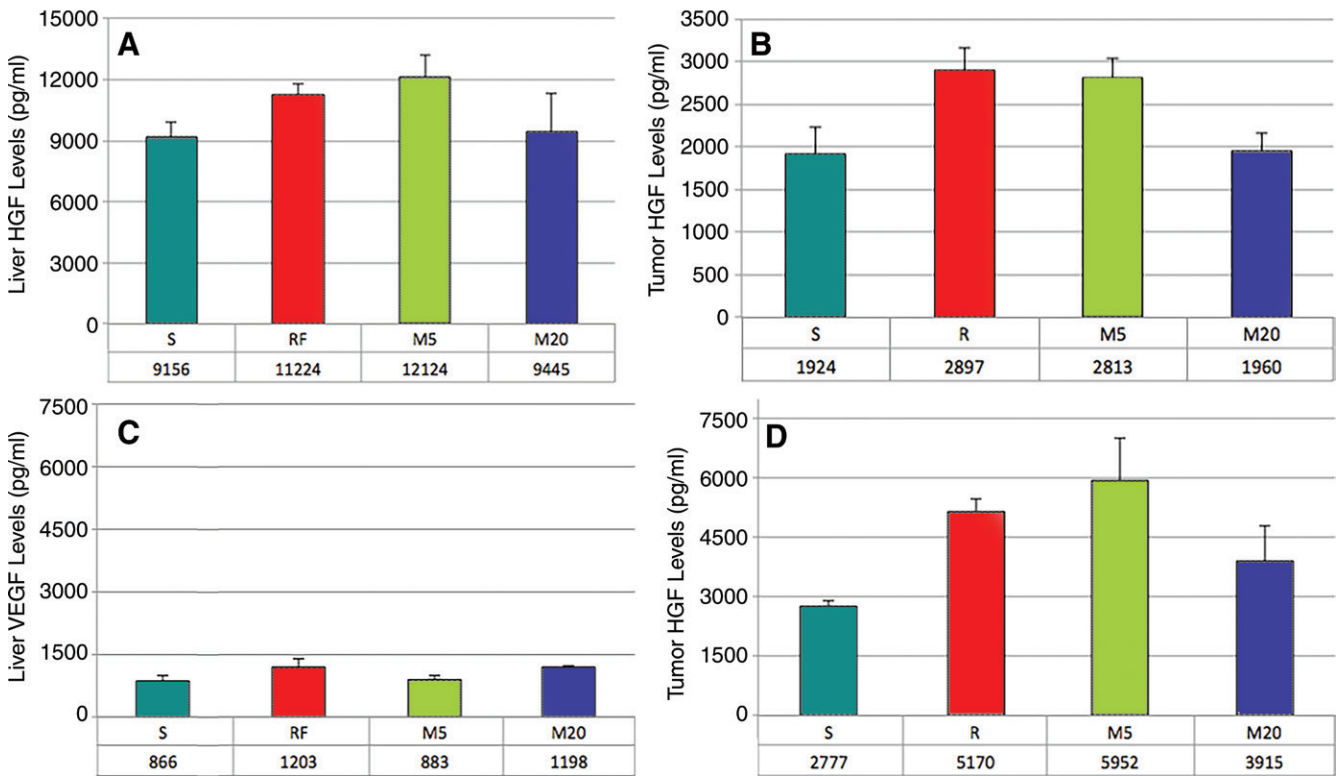


Figure 5: MWA and RFA of normal liver upregulate distant tumor levels of HGF and VEGF. *A, B*, Bar graphs show HGF levels 3 days after liver ablation in, *A*, liver and, *B*, tumor. *C, D*, Bar graphs show VEGF levels 3 days after liver ablation in, *C*, liver, and, *D*, tumor. Similar increases in both liver and tumor HGF levels were seen after lower-power MWA and RFA. No changes were observed between the sham procedure and higher-power MWA energy. Minimal levels of VEGF were detected in the liver after treatment. However, intratumoral levels of VEGF were seen in all treatment arms, with significantly less pronounced effects for higher-power MWA.

Summary of Subcutaneous R3230 Tumor Growth and Proliferative Index after Thermal Ablation of the Normal Liver

Treatment Arm	End Diameter (mm)	Treatment-to-End-Diameter Change (mm)	Preablation Growth Slope	Postablation Growth Slope	Ki-67 Cell Positivity (%)	Microvascular Density*
Sham	13.6 ± 1.3	6.8 ± 0.9	0.60 ± 0.11	0.56 ± 0.15	48.5 ± 5.0	10.6 ± 1.0
RFA	16.3 ± 1.1 [†]	9.3 ± 0.7 [†]	0.60 ± 0.07	0.91 ± 0.11 [†]	78.8 ± 5.0 [†]	15.1 ± 6.7 [†]
5-W MWA	16.3 ± 0.9 [†]	9.5 ± 0.8 [†]	0.62 ± 0.07	0.91 ± 0.14 [†]	81.7 ± 4.7 [†]	17.0 ± 4.4 [†]
20-W MWA	14.6 ± 0.9	7.8 ± 0.6 [†]	0.64 ± 0.02	0.69 ± 0.07	65.0 ± 2.0 [†]	11.3 ± 1.9

Note.—Data are means ± standard deviations. Tumors were followed for 7 days after ablation and were subsequently harvested for quantification of proliferative indexes (percentage Ki-67 cell positivity and CD34 microvascular density).

* Expressed as number of vessels per high-power field.

[†] *P* < .05 when compared with sham group.

no treatment (RFA: 15.4 ± 2.8 and 5-W MWA: 17.1 ± 2.1 vs 20-W MWA: 11.3 ± 1.9 and sham: 10.6 ± 0.9; *P* < .01) (Table). However, no difference was seen between the 20-W MWA and the sham arms (*P* = .30).

Discussion

There is increasing clinical and experimental evidence that percutaneous RFA may stimulate tumor growth separate from the primary ablation site, either

within the same organ or in distant organs. Along these lines, Lencioni et al (1) reported excellent local tumor control in treating solitary HCCs but observed substantially higher rates of new visible tumors at 5 years after RFA than

Figure 6

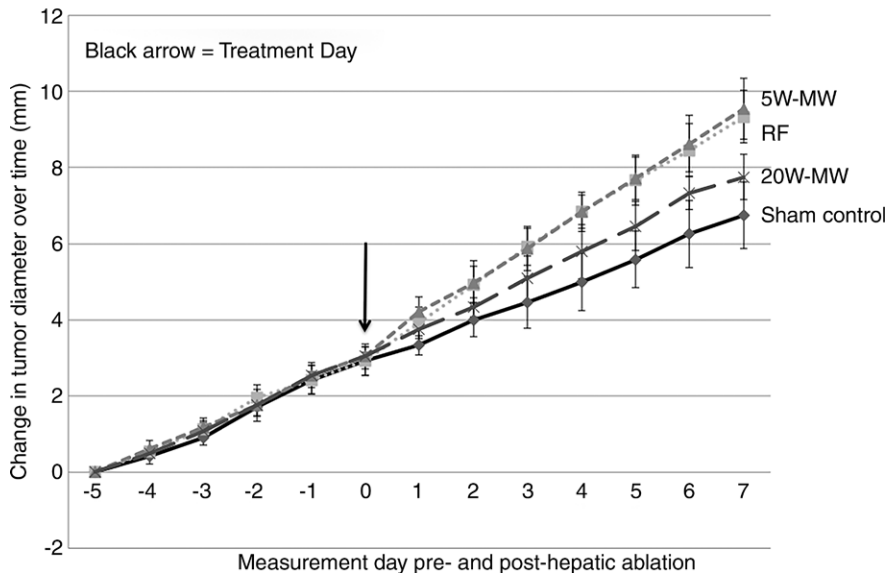


Figure 6: Graph shows that RFA and lower-power MWA of normal liver increase the growth of distant subcutaneous R3230 tumors significantly more than higher-power MWA. Animals implanted with subcutaneous R3230 tumors were treated with hepatic RFA, 5-W MWA, or 20-W MWA. After hepatic ablation (day 0), the growth rates of the distant R3230 tumors significantly increased for RFA and lower-power MWA compared with the sham procedure and higher-power MWA. This resulted in significantly increased tumor size ($P < .05$) at day 7 for RFA and 5-W MWA compared with the sham procedure and 20-W MWA. A significant increase in tumor growth was still seen in higher-power MWA compared with the sham procedure ($P < .05$); however, the effect was much less pronounced.

typically expected in populations that have not undergone hepatic ablation (80% vs 25%–45%) (20). Others have described an increased incidence of intrasegmental tumors after RFA of HCC or more aggressive tumor biology in partially ablated liver tumors (11–13). Periablational inflammation (including IL-6 expression and recruitment of inflammatory cell populations), HSP expression, and growth factor production (eg, HGF/c-Met and VEGF production) have all been implicated as potential contributors to off-target pro-oncogenic effects of RFA (14,18,21,22). Several recent studies have linked increases in posthepatic RFA local inflammation and growth factor production to greater tumorigenesis in animal models of HCC and cirrhosis and of distant subcutaneous breast tumors (12,14,18). Simultaneously, there has been a proliferation of tumor ablation, with alternative energy sources and different mechanisms of tissue injury (5,23,24). However,

the extent to which inflammation and growth factor-mediated pro-oncogenic effects vary between different ablation modalities and whether modification of ablation algorithms can be used to mitigate unwanted effects is unknown.

In our study, we demonstrate that for the same-sized ablation zone, varying the application protocol between a high-power, short-time and a low-power, longer-time application can reduce the extent of periablational partial hyperthermic injury, inflammation, and reactive cytokine and growth factor expression for at least one energy source—MW. One potential explanation for this difference between high- and low-power heating is that with a higher MW energy, heat is being generated throughout the target zone from the interaction of MW energy with tissues directly, while at lower energies, heat is being generated near the probe, and heating within the remainder of the ablation zone (and indeed, at the

margin) is achieved by means of transmission of heat through the adjacent tissue (ie, thermal conduction). This thermal tissue gradient, in turn, may create a wider rim of periablational tissue that is exposed to lower nonlethal levels of heating, similar to what has been described as the “inflammatory rim” or “red zone” in early RFA literature (25,26).

To date, device protocols have been developed to optimize local ablation treatment by maximizing overall ablation size, shortening ablation duration for a given size, or achieving a more spherical ablation geometry (5). However, some approaches, such as lower power ablation with longer heating to achieve greater ablation sphericity, may increase periablational inflammation, as we demonstrate (27). This is particularly relevant given the proliferation of many different ablation platforms in clinical practice and the highly variable application algorithms used—for which any data on the degree to which they incite or reduce periablational inflammation are currently lacking. Thus, given the increasing awareness of regional and systemic off-target effects of hepatic ablation, optimized device algorithms may also need to take these secondary tissue effects into account to maximize overall treatment efficacy, not just ablation zone size or morphology.

We further showed that modifying ablation protocols to reduce local periablational effects and secondary cytokine/growth factor expression can be ultimately used to suppress effects of hepatic ablation on distant tumor growth stimulation. This is an alternative approach to other recent studies that have used targeted molecular inhibition to suppress distant off-target tumor effects (15,18). Recent experimental and clinical studies have implicated pathways linking periablational inflammation, IL-6, HGF/c-Met, and intratumoral VEGF after ablation of both normal and cirrhotic liver to off-target secondary tumorigenic effects (14,28). Here, we demonstrated that distant tumor growth after MWA hepatic ablation is based on similar mechanisms. For both low-power MWA and RFA

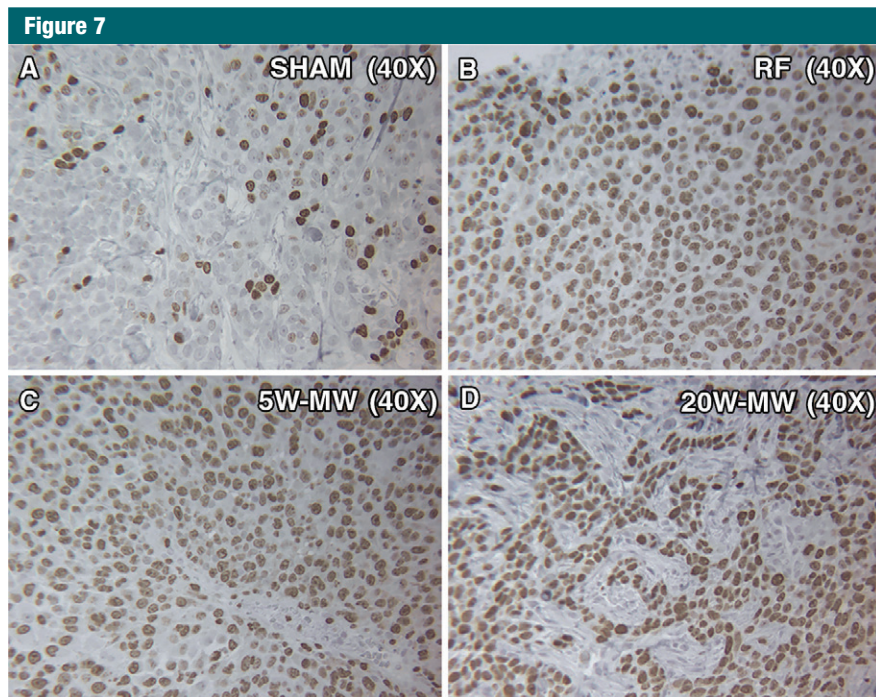


Figure 7: MWA and RFA of normal liver parenchyma cause higher proliferation of distant tumor proliferation at day 7. Representative images of background tumor stained for proliferation marker (Ki-67). Animals were treated with liver ablation with RFA, lower-power MWA, or higher-power MWA and were sacrificed on day 7. Tumors were stained for Ki-67, a proliferation marker of cell division. RFA and lower-power MWA resulted in a higher number of dividing cells (percentage Ki-67 positivity) than the sham procedure and higher-power MWA ($P < .01$).

arms, the degrees of local periablation HSP expression, inflammation, and cytokine/growth factor paralleled each other closely and resulted in similar increased stimulation of distant tumor growth. In our study, higher-power, shorter-duration MWA led to less local periablation inflammation and secondary responses and much less stimulation of distant tumor growth. This is consistent with a prior study that has reported greater periablation rim thickness and serum IL-6 levels for hepatic RFA versus MWA performed with variable ablation protocols (MWA with 20 W \times 2–3 minutes vs RFA with 10 W \times 7–12 minutes) in animals (9). Overall, our study findings strongly suggest that the inflammation-mediated IL-6, VEGF, and HGF-driven effects are based on the heating strategy selected rather than on differences between MW and RF energy alone. Thus, modulation of how ablation is performed,

particularly by using protocols that rapidly achieve ablative effects, may ultimately prove more effective in managing these off-target effects for at least thermal-based therapies.

Our observations of local inflammation, systemic increases in cytokine and growth factor levels, and potential stimulation of distant tumor for two different ablation modalities, RFA and MWA, also support earlier clinical and experimental studies. For example, in 36 patients undergoing ablation of liver, kidney, and lung tumors, Erinjeri et al (16) reported approximately 10-fold and approximately twofold increases in 48-hour postablation serum levels of IL-6 and interleukin-10, respectively, with the highest IL-6 levels observed after cryoablation (50-fold) compared with RFA and MWA (3.5-fold). Recently, in an *Mdr2* knockout model of liver cirrhosis and de novo tumorigenesis, Bulvik et al (29) reported greater

increases in de novo tumorigenesis for irreversible electroporation than for RFA. Thus, our findings may also have direct relevance to other non-thermal ablation modalities, where increased cytokines or tumorigenesis may also be dose dependent.

Finally, we observed many similar trends and changes in the various markers (inflammatory cell recruitment, cytokine and growth factor expression) for hepatic lower-power MWA and RFA, with similar distant tumor growth rates and reduced marker expression with higher-power MWA with relatively less distant tumor growth. This may provide an opportunity to use markers such as IL-6 or c-Met (and potentially others) as surrogate biomarkers to predict the potential for distant tumor stimulation. This approach has been proposed by others, where postablation biopsy of the ablation zone and histopathologic staining for proliferative markers may predict higher rates of tumor recurrence and poorer long-term outcomes (30). In a similar manner, the potential for different ablation modalities, device platforms, and application algorithms to incite off-target effects could be compared by using changes in local or serum levels of key growth factors or cytokines.

There were several limitations to our study. Although these effects were not seen in our study, RFA has also been reported to induce potentially beneficial immunologic effects, including an abscopal effect in some tumor models that can be further enhanced with adjuvant therapies (31–33). Therefore, further studies of the differences between ablation modalities in a wide range of tumor lines and types (particularly those that demonstrate abscopal effects after RFA) are needed to determine those circumstances in which modification of ablation parameters can be used to augment antitumor immunity. Additionally, all the ablations in our study were performed in only one tissue type, normal liver (as this closely simulates the clinical practice of achieving an ablative margin), and only one tumor model, subcutaneous in situ breast tumors. Although similar findings after hepatic RFA for

other tumor types (de novo HCC in inflammatory cirrhosis in the *Mdr2* knockout mouse model) and organs (eg. the kidney) have already been reported, additional verification will be required for MWA in other settings to understand the true clinical impact of our study's findings. Furthermore, we acknowledge that each ablation energy source can be applied using numerous applicator designs and with a multitude of energy parameters, including durations and intensities. All of these may potentially affect the outcomes of the treatments, both in terms of the ablation size and the extent of inflammation produced. Thus, although the duration and intensities of RFA and MWA used in this study accurately reflect a reasonable range of applications and MW frequencies in clinical settings, further study is likely warranted (5,34). Finally, especially in light of the unexplained elevation in activated myofibroblasts seen for lower-energy MW, we acknowledge that our understanding of all of the differences in postablation reactions for the different ablation strategies is currently incomplete and that further mechanistic study is likely warranted.

In summary, thermal ablation of normal liver parenchyma, regardless of energy source used, can incite systemic inflammatory reactions and increase distant tumor growth, although modifying the heating strategy toward higher-power, shorter-duration ablation can be used to reduce periablation inflammation and associated off-target effects in the short term. This suggests that modifying ablation protocols along these lines may offer an opportunity to reduce unwanted stimulation of distant tumor growth in some clinical cases. However, further understanding of the underlying mechanisms behind ablation-induced tumorigenesis is needed to determine which tumors and patients are likely to benefit from this approach.

Disclosures of Conflicts of Interest: E.V. disclosed no relevant relationships. S.N.G. Activities related to the present article: none to disclose. Activities not related to the present article: is a consultant for Cosman and Angiodynamics. Other relationships: none to disclose. G.K. disclosed no relevant relationships. Y.W.

disclosed no relevant relationships. S.G. disclosed no relevant relationships. J.S. disclosed no relevant relationships. T.M. disclosed no relevant relationships. C.L.B. Activities related to the present article: none to disclose. Activities not related to the present article: is a consultant for NeuWave Medical and Symple Surgical; receives money from patents and royalties from the Wisconsin Alumni Research Foundation; holds stock in NeuWave Medical. Other relationships: none to disclose. M.A. disclosed no relevant relationships.

References

- Lencioni R, Cioni D, Crocetti L, et al. Early-stage hepatocellular carcinoma in patients with cirrhosis: long-term results of percutaneous image-guided radiofrequency ablation. *Radiology* 2005;234(3):961-967.
- Meloni MF, Andreano A, Laeseke PF, Livraghi T, Sironi S, Lee FT Jr. Breast cancer liver metastases: US-guided percutaneous radiofrequency ablation—intermediate and long-term survival rates. *Radiology* 2009;253(3):861-869.
- Solbiati L, Ahmed M, Cova L, Ierace T, Brischio M, Goldberg SN. Small liver colorectal metastases treated with percutaneous radiofrequency ablation: local response rate and long-term survival with up to 10-year follow-up. *Radiology* 2012;265(3):958-968.
- El-Serag HB. Hepatocellular carcinoma. *N Engl J Med* 2011;365(12):1118-1127.
- Ahmed M, Brace CL, Lee FT Jr, Goldberg SN. Principles of and advances in percutaneous ablation. *Radiology* 2011;258(2):351-369.
- Goldberg SN, Gazelle GS, Mueller PR. Thermal ablation therapy for focal malignancy: a unified approach to underlying principles, techniques, and diagnostic imaging guidance. *AJR Am J Roentgenol* 2000;174(2):323-331.
- Wells SA, Hinshaw JL, Lubner MG, Ziemlewicz TJ, Brace CL, Lee FT Jr. Liver ablation: best practice. *Radiol Clin North Am* 2015;53(5):933-971.
- Brace CL. Microwave tissue ablation: biophysics, technology, and applications. *Crit Rev Biomed Eng* 2010;38(1):65-78.
- Ahmad F, Gravante G, Bhardwaj N, et al. Changes in interleukin-1 β and 6 after hepatic microwave tissue ablation compared with radiofrequency, cryotherapy and surgical resections. *Am J Surg* 2010;200(4):500-506.
- Ahmad F, Gravante G, Bhardwaj N, et al. Renal effects of microwave ablation compared with radiofrequency, cryotherapy and surgical resection at different volumes of the liver treated. *Liver Int* 2010;30(9):1305-1314.
- Nijkamp MW, van der Bilt JD, de Bruijn MT, et al. Accelerated perinecrotic outgrowth of colorectal liver metastases following radiofrequency ablation is a hypoxia-driven phenomenon. *Ann Surg* 2009;249(5):814-823.
- Rozenblum N, Zeira E, Bulvik B, et al. Radiofrequency ablation: inflammatory changes in the periablation zone can induce global organ effects, including liver regeneration. *Radiology* 2015;276(2):416-425.
- Nikfarjam M, Muralidharan V, Christophi C. Altered growth patterns of colorectal liver metastases after thermal ablation. *Surgery* 2006;139(1):73-81.
- Rozenblum N, Zeira E, Scaiewicz V, et al. Oncogenesis: an "off-target" effect of radiofrequency ablation. *Radiology* 2015;276(2):426-432.
- D'Ipollito G, Ahmed M, Girmun GD, et al. Percutaneous tumor ablation: reduced tumor growth with combined radio-frequency ablation and liposomal doxorubicin in a rat breast tumor model. *Radiology* 2003;228(1):112-118.
- Erinjeri JP, Thomas CT, Samoilia A, et al. Image-guided thermal ablation of tumors increases the plasma level of interleukin-6 and interleukin-10. *J Vasc Interv Radiol* 2013;24(8):1105-1112.
- Wang X, Sofocleous CT, Erinjeri JP, et al. Margin size is an independent predictor of local tumor progression after ablation of colon cancer liver metastases. *Cardiovasc Intervent Radiol* 2013;36(1):166-175.
- Ahmed M, Kumar G, Navarro G, et al. Systemic siRNA nanoparticle-based drugs combined with radiofrequency ablation for cancer therapy. *PLoS One* 2015;10(7):e0128910.
- Ahmed M, Kumar G, Moussa M, et al. Hepatic radiofrequency ablation-induced stimulation of distant tumor growth is suppressed by c-Met inhibition. *Radiology* 2016;279(1):103-117.
- Mittal S, El-Serag HB. Epidemiology of hepatocellular carcinoma: consider the population. *J Clin Gastroenterol* 2013;47(Suppl):S2-S6.
- Harun N, Costa P, Christophi C. Tumor growth stimulation following partial hepatectomy in mice is associated with increased upregulation of c-Met. *Clin Exp Metastasis* 2014;31(1):1-14.
- Xie B, Xing R, Chen P, et al. Down-regulation of c-Met expression inhibits human HCC cells growth and invasion by RNA interference. *J Surg Res* 2010;162(2):231-238.

23. Wendler JJ, Ricke J, Pech M, et al. First delayed resection findings after irreversible electroporation (IRE) of human localised renal cell carcinoma (RCC) in the IRENE Pilot Phase 2a Trial. *Cardiovasc Intervent Radiol* 2016;39(2):239–250.
24. Chinnaratha MA, Chuang MA, Fraser RJ, Woodman RJ, Wigg AJ. Percutaneous thermal ablation for primary hepatocellular carcinoma: a systematic review and meta-analysis. *J Gastroenterol Hepatol* 2016;31(2):294–301.
25. Mertyna P, Dewhirst MW, Halpern E, Goldberg W, Goldberg SN. Radiofrequency ablation: the effect of distance and baseline temperature on thermal dose required for coagulation. *Int J Hyperthermia* 2008;24(7):550–559.
26. Mertyna P, Goldberg W, Yang W, Goldberg SN. Thermal ablation: a comparison of thermal dose required for radiofrequency-, microwave-, and laser-induced coagulation in an ex vivo bovine liver model. *Acad Radiol* 2009;16(12):1539–1548.
27. Hoffmann R, Rempp H, Erhard L, et al. Comparison of four microwave ablation devices: an experimental study in ex vivo bovine liver. *Radiology* 2013;268(1):89–97.
28. Hinz S, Tepel J, Röder C, Kalthoff H, Becker T. Profile of serum factors and disseminated tumor cells before and after radiofrequency ablation compared to resection of colorectal liver metastases: a pilot study. *Anticancer Res* 2015;35(5):2961–2967.
29. Bulvik BE, Rozenblum N, Gourevitch S, et al. Irreversible electroporation versus radiofrequency ablation: a comparison of local and systemic effects in a small-animal model. *Radiology* 2016;280(2):413–424.
30. Sofocleous CT, Garg S, Petrovic LM, et al. Ki-67 is a prognostic biomarker of survival after radiofrequency ablation of liver malignancies. *Ann Surg Oncol* 2012;19(13):4262–4269.
31. Behm B, Di Fazio P, Michl P, et al. Additive antitumor response to the rabbit VX2 hepatoma by combined radio frequency ablation and toll like receptor 9 stimulation. *Gut* 2016;65(1):134–143.
32. Kroeze SG, Daenen LG, Nijkamp MW, et al. Radio frequency ablation combined with interleukin-2 induces an antitumor immune response to renal cell carcinoma in a murine model. *J Urol* 2012;188(2):607–614.
33. Nakagawa H, Mizukoshi E, Iida N, et al. In vivo immunological antitumor effect of OK-432-stimulated dendritic cell transfer after radiofrequency ablation. *Cancer Immunol Immunother* 2014;63(4):347–356.
34. Poulou LS, Botsa E, Thanou I, Ziakas PD, Thanos L. Percutaneous microwave ablation vs radiofrequency ablation in the treatment of hepatocellular carcinoma. *World J Hepatol* 2015;7(8):1054–1063.